

# Activity identification and classification in wheelchair rugby using fractal dimensions

Julian J. C. Chua<sup>1</sup> · Franz Konstantin Fuss<sup>1</sup> · Aleksandar Subic<sup>2</sup>

© International Sports Engineering Association 2016

**Abstract** The purpose of the study was to develop an evidence-based method for identification and classification of wheelchair sports (rugby) activities and performance during a match using fractal dimensions. The approach involves five wheelchair rugby athletes of different classifications who were monitored during six different matches using mobile devices with in-built accelerometers. The linear acceleration signals were processed using two different approaches based on calculating fractal dimensions. One was based on Rényi's entropy, which produced the probability dimension ( $S_0$ ), and the other was based on Hausdorff's definition, resulting in the Hausdorff dimension ( $D_H$ ). When both dimensions were individually plotted as cumulative distribution plots, they offered two approaches to analyze the performance of a wheelchair rugby athlete. Combining the two dimensions produced a two-dimensional (2D) mapping that identified five different activities of each athlete during a wheelchair rugby match—(1) no activities, (2) low activities, (3) high-speed coasting, (4) high-speed pushing, and (5) extreme collisions. In the 2D mapping, four boundary lines separate the five different activities, which produced a template for each athlete. It was found in this research that the classification and skill level of the athlete had an effect on the boundary

line values that form the template. The outcome of the activity identification was also verified by comparing with video footage of the athletes. The method developed in this research has possible applications for coaching, match analysis, and talent identification.

**Keywords** Accelerometer · Fractal dimensions · Hausdorff dimension · Disability sports · Performance analysis · Activity analysis · Wheelchair · Wheelchair rugby

## 1 Introduction

Tracking the activities and performance parameters of wheelchair rugby athletes during a match can provide greater insight into the game dynamics and athletes' efforts [1]. Many studies have attempted to track wheelchair rugby athletes during a match using miniaturized data loggers [2], video cameras and image-processing techniques [3], and indoor wireless tracking system [1, 4]. However, none of them looked at identifying specific match activities. A method that identifies specific activities is the Game Efficiency Sheet [5, 6], which tracks athletes' activities, such as number of passes, blocks, turnovers, steals, and scores. However, this basically requires a team of reviewers to manually note down each of those activities, very labor intensive, and time consuming.

In an elite rugby league, able-bodied athletes are typically fitted with inertia measurement units (IMU), which are built with triaxial accelerometers, gyroscopes, magnetometers, and GPS modules [7]. This provides position data of the athletes, while the accelerometers and gyroscopes provide information on physical collisions and repeated high-intensity efforts [8]. The accelerometer data from the

✉ Franz Konstantin Fuss  
franz.fuss@rmit.edu.au

Julian J. C. Chua  
julianchua@gmail.com

<sup>1</sup> School of Aerospace, Mechanical and Manufacturing Engineering, RMIT University, GPO Box 2476, Melbourne, VIC 3001, Australia

<sup>2</sup> Swinburne Research, Swinburne University of Technology, Melbourne, Australia

athletes' movements are used to calculate a performance parameter called Player Load. This parameter has been validated and can be used to estimate the physical demands and, thus, performance of the athlete [9]. However, there are no such performance parameters developed for wheelchair rugby athletes to identify the level of activity or performance.

In terms of quantifying performance, wheelchair rugby, which is considered a non-rhythmic type of activity, cannot adopt the same methods used for rhythmic activities, such as walking, swimming, and running. For rhythmic activities, stroke frequencies do not significantly change over time, so performance can be quantified by identifying individual strokes, locating the stroke peaks, counting the strokes, and measuring the amplitude and time between strokes [10]. For non-rhythmic activities, cumulative activity analysis might be more appropriate, as it is based on mean accelerometer counts per minute and allows for semi-qualitative assessment. For example: using accelerometers to measure physical activity in young children, and classifying them into five categories—sedentary, light, moderate, moderate-to-vigorous, and vigorous activity [11]; or just monitoring moderate-to-vigorous physical activity (MVPA) [12, 13].

An alternative to quantifying performance through calculating mean accelerometer counts per minute is fractal analysis of acceleration data. Fractal geometry of signals has been applied extensively for electric activity analysis of EEG signals [14–18]. In sport climbing, fractal analysis based on a probability distribution method [15] was applied on force–time data and the results showed a strong correlation between fractal dimension and conventional performance parameters [19]. Using the same fractal analysis method, linear acceleration of four manual wheelchair push patterns was analyzed; and it was found that fractal dimensions of the acceleration signal were useful for distinguishing the four push patterns [20]. However, the fractal dimensions calculated with this algorithm are highly dependent on signal amplitude and impulse. A subsequent study applied a slightly similar concept to distinguish five different activities of a paralympic wheelchair rugby athlete which were: (1) no activity, (2) low-level activity, (3) high-speed coasting, (4) high-speed pushing, and (5) collisions [21]. The method used to derive fractal dimensions was according to Hausdorff [22]. Plotting the fractal dimensions against the average acceleration amplitudes of the five activities produced two-dimensional map that showed a clear distinction between the five activities; and this proved to be a useful method for identifying and classifying wheelchair rugby activities. However, it was noted that the average amplitude method is not ideal due to its high standard deviation. It was also noted that the

window width size of the running average procedure had a notable effect on the fractal dimensions.

The objectives of this study are four-fold: first, to develop the activity identification and classification method using two-dimensional mapping, the proposed method is to apply and combine two fractal analysis methods—one based on Hausdorff's dimension ( $D_H$ ) [23] and another based on probability distribution or Renyi's entropy [24] which was applied previously to distinguish four different manual wheelchair push patterns [20]; second, to ensure that the boundary lines (separating the ranked activities) determined from the two-dimensional mapping are accurate, this is achieved through a sensitivity analysis; third, to optimize the above two-dimensional mapping by determining the optimum window width size and the optimum amplitude multiplier for calculating  $D_H$ ; and finally, to apply the above to real match data of wheelchair rugby athletes of various classifications and to analyze the outcomes in terms of how it could support coaches and sports scientists.

## 2 Calculating fractal dimensions

Two methods of calculating fractal dimensions were applied in this study.

The first method is the fractal dimension based on Hausdorff's definition or simply Hausdorff dimension,  $D_H$  [22]. It is defined as the most efficient covering of irregular curves and surface profiles, usually approximated by boxes or circles or yardsticks. The most basic way of describing the method is where an irregular curve is covered by  $N$  number of either boxes of size  $r$ , circles of radius  $r$ , or rulers of length  $r$ .

$$D_H = \lim_{r \rightarrow 0} \frac{\log N}{\log 1/r}. \quad (1)$$

From this basic principle, there are variations to how an irregular curve can be covered. The approach taken in this study is a method developed by Fuss [23], which combines Katz' euclidean length of a signal [25] and Higuchi's rate of change of log length with respect to log frequency [26].

Fuss' generalized formula [23] for calculating relative lengths of the varying sampling frequencies with window width,  $w$ , start datum of window,  $j$ , and multiplier of period,  $k$  (where  $k = 1, 2, 4, \dots$ ) is:

$$R_{j,w,k} = \frac{1}{k} \left[ \sum_{i=j}^{j+w-k} R_i + \sum_{l=1}^k \frac{k-l}{k} (R_{j-l} + R_{j+w-k+1}) \right] \quad (2)$$

and

$$R_i = \frac{f_0 L_i}{k} \quad (3)$$

$$L_i = \sqrt{m^2(y_{i+k} - y_i)^2 + \left(\frac{k}{f_0}\right)^2} \quad (4)$$

where  $L_i$  is the segment length,  $f_0$  is the original sampling frequency,  $y$  is the acceleration data, and  $m$  is the amplitude multiplier.

Finally, the Hausdorff dimension,  $D_H$  is:

$$D_H = \lim_{k \rightarrow 0} \frac{\log R_{j,w,k}}{\log f_0/k}. \quad (5)$$

The second method is the probability distribution method based on Rényi's generalized dimension,  $D_q$ . It can be defined as:

$$D_q = \lim_{r \rightarrow 0} \frac{1}{1-q} \frac{\log \sum_{i=1}^N p_i^q}{\log 1/r} \quad (6)$$

which covers the entire fractal spectrum for  $-\infty < q < +\infty$ . It can be called the  $q$ th-order fractal dimension. The numerator is the generalized Rényi entropy  $S_q$  [27] which is the spectrum of a probability distribution:

$$S_q = \frac{1}{1-q} \log \sum_{i=1}^N p_i^q \quad (7)$$

where  $p_i$  is the probability of having a point in the  $i$ th bin, and  $p_i = N_i/N$  with  $N_i$  being the number out of a total  $N$  points in the  $i$ th bin.

When  $q = 0$ , Eq. (6) becomes the fractal dimension  $D_0$ :

$$D_0 = \lim_{r \rightarrow 0} \frac{\log N_0}{\log 1/r} \quad (8)$$

where  $N_0$  represents the number of occupied bins and  $1/r$  is the resolution of the sensor, as recommended by [15].

In the analysis of EEG as a fractal time series [15] as well as manual wheelchair push patterns [20], the authors did not apply a limit to  $r$ . Strictly speaking, that will only be considered a fractal dimension if the signals were perfectly self-similar [28]. However, in the cases where signals are not perfectly self-similar, it will be more appropriate to use the notation  $S_0$  and the term 'probability dimension' to avoid confusion. Therefore, in this case, the probability dimension,  $S_0$ , is:

$$S_0 = -\frac{\log N_0}{\log 1/r}. \quad (9)$$

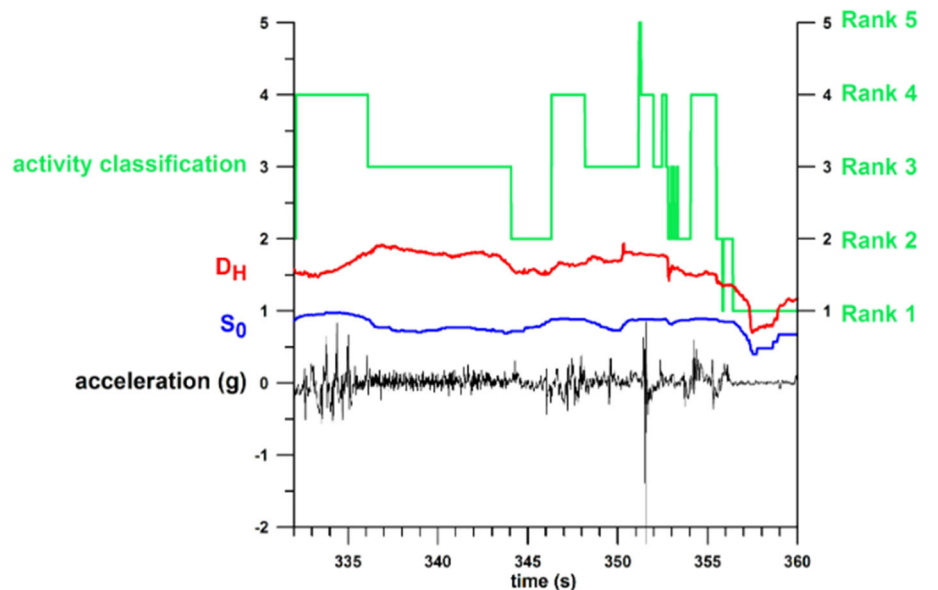
Continuous  $S_0$  and  $D_H$  of acceleration-time data (Fig. 1) were calculated using a sliding window method. The sliding window concept is similar to applying a running average filter, but instead of the average,  $S_0$  and  $D_H$  were calculated across the window. There are two parameters in the above calculations that require optimization and they are the window width,  $w$ , and amplitude multiplier,  $m$ . Adjusting  $w$  and  $m$  affects the values of  $S_0$  and  $D_H$  and, subsequently, the effectiveness of the activity identification. This will be discussed further in Sect. 3.

## 3 Methodology

### 3.1 Overview

First, acceleration data of the wheelchair rugby athletes and video were captured from actual wheelchair rugby matches. Then,  $S_0$  and  $D_H$  of the acceleration data were calculated.  $S_0$  and  $D_H$  were then used to derive performance

**Fig. 1** Plot of acceleration against time, its corresponding  $S_0$  and  $D_H$  plots, and activity classification levels



and activity classification curves. They were also used together with video data to perform activity identification followed by 2D mapping, and that produced the Decision Template for each athlete. The Decision Template identifies and quantifies the five main activities. After completing those steps for one match quarter data, an optimization was executed to select the best  $w$  and  $m$  values. A range of  $w$  and  $m$  values were tested to determine different sets of  $S_0$  and  $D_H$  and different activity identification outcomes. Optimum  $w$  and  $m$  values were selected, such that the activity identification is most effective. The optimum values were then used to compute  $S_0$  and  $D_H$  of the remaining match quarter data, followed by computing the Decision Templates and the performance and activity classification curves. Figure 2 shows the process flow for all the main steps.

### 3.2 Data collection

Linear acceleration data of the wheelchair rugby athletes were captured using mobile devices (Model: A1367, Apple Inc, Cupertino CA, USA). They were mounted on the athletes customized rugby wheelchairs during six different matches of the Victorian Wheelchair Rugby League. Five athletes from the three different classes (high-pointer, mid-pointer, and low-pointer) volunteered to have their acceleration measured. The athletes were fully informed of the research procedures and potential risks, and written consent was obtained from all research participants. Ethics approval (Number: ASEHAPP 01-11) was obtained from the RMIT University Human Research Ethics Committee prior to the experimental study. The acceleration data were recorded at 60 Hz.

**Fig. 2** Process flow for determining the decision template and activities ranking for each athlete

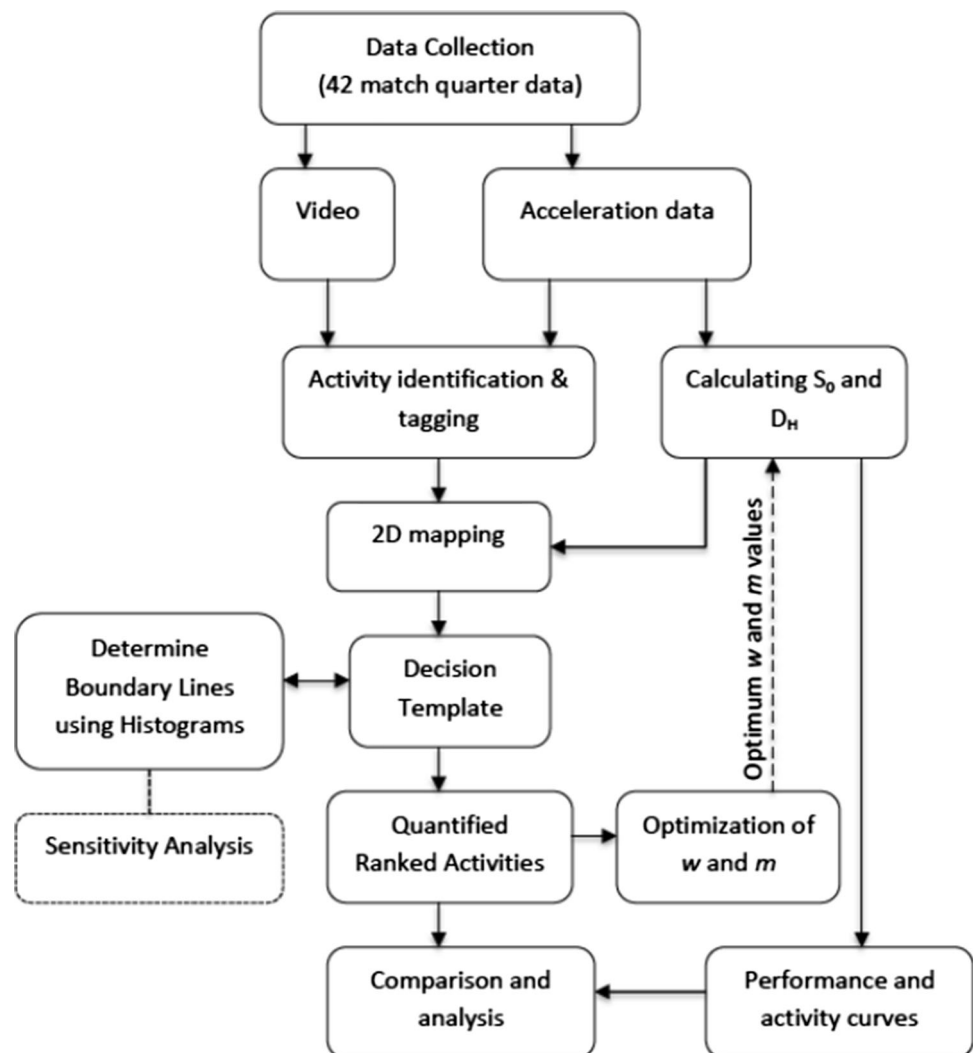


**Table 1** List of wheelchair rugby athletes, the number of full match quarters they participated in and their boundary line values for activity classification.

Athlete code	Class (classification points)	Highest level played	Matches numbers (M1–6) and numbers of full match quarters played by athlete						Boundary lines/decision template			
			M1	M2	M3	M4	M5	M6	A	B	C	D
HP1	High-pointer (3)	Paralympic games	2	4	0	0	<b>3</b>	<b>4</b>	0.88	1.33	1.5	1.73
MP1	Mid-pointer (2)	Paralympic games	0	0	0	4	<b>0</b>	<b>4</b>	0.845	1.31	1.55	1.725
MP2	Mid-pointer (2)	National league	0	0	4	0	<b>4</b>	<b>0</b>	0.84	1.275	1.46	1.73
LP1	Low-pointer (0.5)	National league	0	0	4	4	<b>0</b>	<b>0</b>	0.785	1.195	1.395	1.65
LP2	Low-pointer (0.5)	State league	0	0	0	0	<b>3</b>	<b>2</b>	0.74	1.185	1.42	1.72

Matches (M5 and M6) identified in bold font comprise of data for three athletes

The mobile devices were embedded into rectangular foam blocks before being secured onto each athlete's wheelchair frame to protect them from possible direct impacts. The mounting of the devices was unobtrusive and did not affect the athletes' movements. Video footage was also captured using a Sony HDR-CX110E camcorder for verifying the activities of the athletes and synchronizing the acceleration data of athletes in the same match.

The athletes consist of a high-pointer (HP1), two mid-pointers (MP1 and MP2), and two low-pointers (LP1 and LP2). The athletes' details and the numbers of full match quarters played are shown in Table 1, and there were a total of 42 full match quarters.

### 3.3 2D mapping and decision template

Five main activities are typically present in a wheelchair rugby match [21], ranked 1–5:

- Rank 1. No activity
- Rank 2. Low activity—including low-speed pushing, low-speed coasting and turns
- Rank 3. High-speed coasting
- Rank 4. High-speed pushing
- Rank 5. Extreme collisions.

Not every activity of the wheelchair rugby athlete can be easily classified under one of these five activities. However, instances that obviously fall under these categories were identified from the video footage. Acceleration data of those instances were tagged with the associated rank numbers of between 1 and 5. The corresponding  $S_0$  and  $D_H$  data were then plotted against each other, as shown in Fig. 3 with each ranked activity plotted with a different colour. It can be seen that there is a separation between the five activities that can be specified by four boundary lines—A, B, C, and D. The four lines form a decision template that can be applied to all the acceleration data of the quarter, so that every activity can be classified. The exact value of the boundary lines location should be determined using histogram plots instead of visual inspection, which would be highly inaccurate.

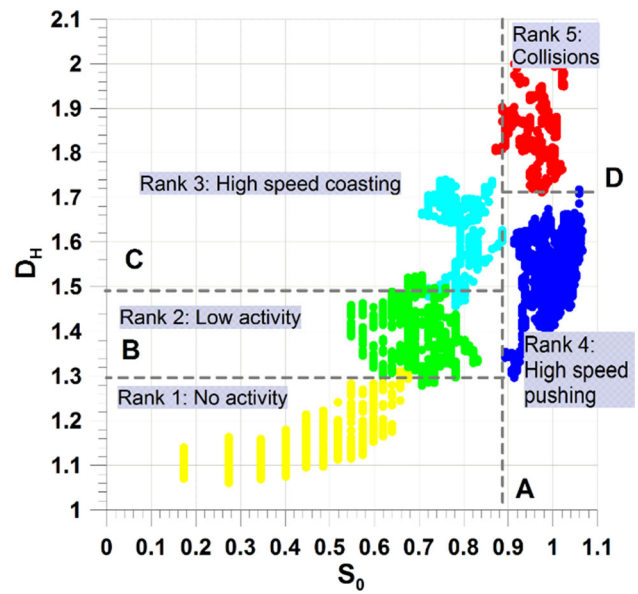


**Fig. 3** Plot of  $D_H$  against  $S_0$ , and the boundary lines (A, B, C, D) that form the decision template

#### 3.3.1 Boundary line histograms and sensitivity analysis

For each boundary line (A, B, C, or D), the data that are separated by the line were grouped together, so there is one group of data on each side of the boundary line. These two groups of data are plotted as histogram plots, as shown in Fig. 4. As illustrated in that graph, each histogram plot has a 'rapid drop' point, and the mid-point between the two 'rapid drop' points is selected as the boundary line value. In most cases, the mid-point coincided with the intersection of the Gaussian curves of the two activity distributions evaluated.

Furthermore, a sensitivity analysis was conducted to emphasize the importance of accurately determining the boundary lines' values. For the sensitivity analysis, first, the four boundary lines for an athlete were obtained using the histogram method and, thus, obtaining the decision template; this was followed by classifying all the match



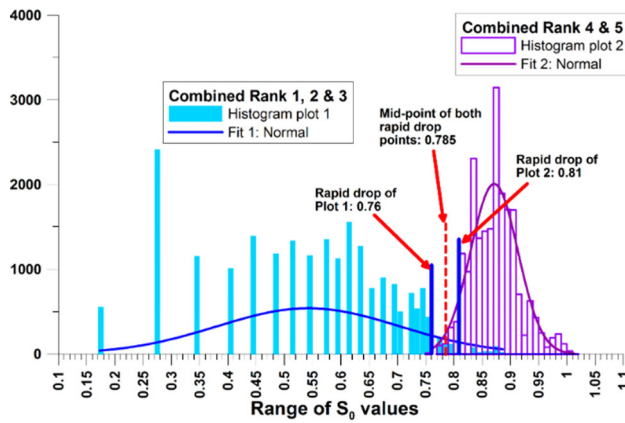


**Fig. 4** Histogram plot applied to accurately determine the value of boundary line A

quarter data using the decision template and plotting all the amount of the five classified activities onto a pie chart. Next, each boundary line value was adjusted by  $\pm 1\%$  and the change in amount of activities due to that adjustment was noted. The outcome showed that a slight shift in the boundary line values had a much greater effect in the shift in amount of activities, especially for boundary line A.

### 3.4 Optimization of $w$ and $m$

#### 3.4.1 Window width optimization

Previous studies have discussed the influence of window width on the effectiveness of the fractal dimension derived. Window widths that are too small may result in too much noise in the fractal dimension [29]. However, if the window width is too wide, it could miss out key activities or information [30]. Therefore, selecting an optimum window width regulated the  $S_0$  and  $D_H$  values for a more accurate identification of wheelchair rugby activities using the Decision Template. The percentage change in the level of each ranked activity should be minimal at the optimum window width.  $S_0$  and  $D_H$  values calculated using the optimum width will not be too noisy or over-filtered.

The optimization was carried out by testing out a range of window widths from 0.5 to 5 s (0.5, 1.0, 1.5, 2.0, 2.5, 3.0, 3.5, 4.0, and 5.0), or at a sampling rate of 60 Hz, and window width of 30–300 data points. The nine different window widths were applied to calculate  $S_0$  and  $D_H$  for acceleration data from one match quarter. At the same time, the acceleration data were tagged with the five ranked activities, and the Decision Template was created for that athlete, so that all instances within the match quarter were classified into the five activities. Two comparisons were carried out to see the effect of window width adjustment:

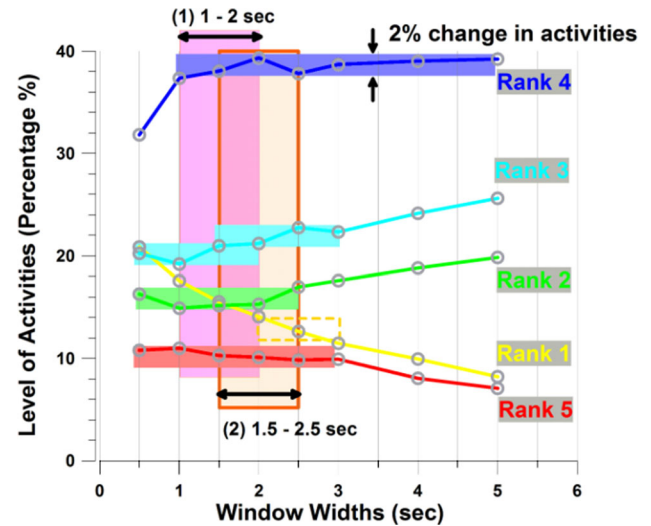


**Fig. 5** Percentage change in level of activities with varying window widths

1. Differences in the  $S_0$  and  $D_H$  data
2. Differences (percentage changes) in the distribution of activity classification.

The window width range that displays the most stable level of activities in all five ranks is the optimum  $w$ . Looking at Fig. 5, the change in level of activities as window width was varied. By applying a filter that marks out changes not more than 2% in terms of activities, two regions of window widths appeared to be most stable ones for Rank 2–4 activities: (1) the 1–2 s window width and (2) the 1.5–2.5 s window width. Since the cumulative activity time of Rank 1 (no activity) was overestimated at smaller window width (when comparing the calculated activity to the actual signal), a 2.5 s window width was selected for processing. Furthermore, comparing the effect of the nine window widths on  $S_0$  and  $D_H$  against time, it was noted that the largest window width (5 s) acted like a filter, cutting off the peaks in both  $S_0$  and  $D_H$ . On the other hand, the smallest window width (0.5 s) gave  $D_H$  better resolution or greater range, but also increased the amount of noise in both  $S_0$  and  $D_H$  data. Therefore, the 2.5 s window width was suitable for reducing excessive noise in  $S_0$  and  $D_H$ , while not cutting off peaks, which is important for identifying activities.

#### 3.4.2 Amplitude multiplier optimization

Equation (4) shows the amplitude multiplier,  $m$ , used for scaling and modifying the signal's amplitude. The objective of optimizing the amplitude multiplier,  $m$ , is similar to optimizing the window width, specifically to optimize the range of values of  $D_H$  in terms of:

- Clearer separation of the five different wheelchair rugby activities for decision making; and
- Maximising the difference in  $D_H$  of rank 1 (no activity; smallest  $D_H$ ) and rank 5 (extreme collisions; highest  $D_H$ ).

Nine amplitude multiplier values (from  $10^{-2.5}$ – $10^4$  in steps of  $10^{0.5}$ ) were applied to the same match quarter acceleration data which gave nine sets of  $D_H$  values. They were then compared to find the optimum multiplier value.

The optimization process was as follows:

1. For each set of  $D_H$  data, the following parameters were determined: maximum value,  $D_{Hmax}$ , minimum value,  $D_{Hmin}$ ,  $D_{Hrange}$  ( $D_{Hmax} - D_{Hmin}$ ), and  $D_{Hmean}$  ( $(D_{Hmax} + D_{Hmin})/2$ ). Then, based on these values, the conditions for an optimum  $m$  value are:
  - Maximized range ( $D_{Hmax} - D_{Hmin}$ ) value ( $D_H$  differential).
  - $D_{Hmax} \leq 2$ .
  - $D_{Hmin} \geq 1$ .
2. The different sets of  $D_H$  data were plotted against time and compared with the acceleration signal for usability. In this case, different types of accelerations should be reflected in the  $D_H$  values.

Plotting  $D_H$  against  $\log m$  shows that both  $D_{Hmax}$  and  $D_{Hmin}$  reach asymptotic values of  $D_H = 1$  and  $D_H = 2$  (Fig. 6) at small and large  $m$ , respectively, such that the  $D_H$

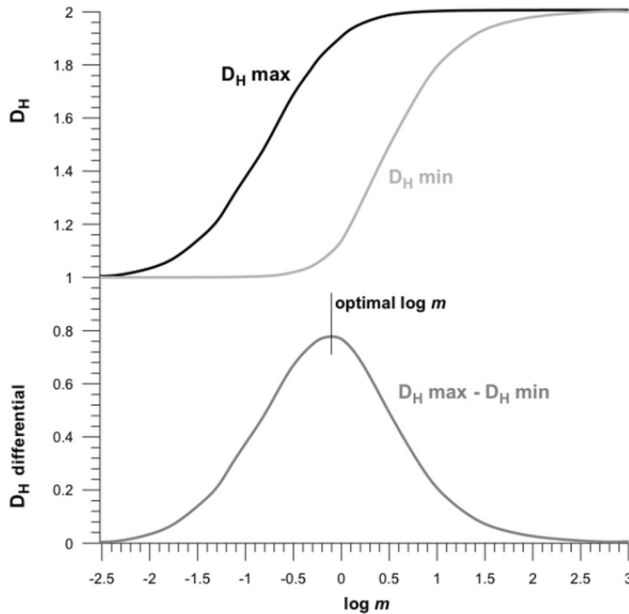


**Fig. 6** Plots of  $D_{Hmax}$  (Rank 5, extreme collisions),  $D_{Hmin}$  (Rank 1, no activity), and  $D_{Hrange}$  ( $D_H$  differential) against  $\log m$

differential approached zero. The  $D_H$  differential was at its maximum at  $m = 0.8$  (or  $\log m = -0.097$ ). As the optimal  $m$  value was close to 1, and as the  $D_H$  differential at  $m = 1$  was only 1.16 % smaller than the optimal  $D_H$  differential, the acceleration signal's amplitude (unit =  $g$ ) was left unchanged ( $m = 1$ ). If, however, the amplitude's unit was  $\text{ms}^{-2}$ , then the optimal multiplier,  $m$ , would have been  $m \approx 0.08$ .

Plotting several sets of  $D_H$  values and acceleration data against time, the optimum set of  $D_H$  values was the one with unit multiplier. For amplitude multiplier values more or less than unity, the  $D_H$  differential decreased and was, therefore, not ideal for separating and identifying between different activities. Multipliers higher than unity were not ideal for separating activities, because they resulted in higher  $D_H$  values for “low-level activities” (Rank 2) which in some cases were higher than “high-speed pushing” (Rank 4). On the other hand,  $D_H$  with multiplier, ‘1’, had lower values for “no activity” (Rank 1) and “low-level activities” (Rank 2); and higher values for “high-speed pushing” (Rank 4) and “extreme collisions” (Rank 5). This is also clearly explained in [23].

### 3.5 Performance and activity classification curves

Wheelchair rugby is played in quarters with each quarter lasting 8 min. Since athletes do not play for all four quarters of a match especially at the elite level which is the Paralympic games, it is logical to quantify match performance and activities by each quarter.

The performance curve of each match quarter data is derived by first obtaining the probability density function of  $S_0$ , followed by the cumulative distribution (Fig. 7). Likewise, the activity classification curve (or activity curve) of each match quarter is the cumulative distribution plot of  $D_H$ .

The cumulative plot of  $S_0$  was termed the performance curve, because  $S_0$  relates to energy released into the environment as a result of effort which the athlete put in [31].  $S_0$  is directly related to the mean peak acceleration amplitude, whereas the cumulative plot of  $D_H$  was termed the activity curve, because  $D_H$  is related to how the acceleration signal fills up each window width, which is influenced by a combination of push pattern and type of wheelchair activity.

The performance curve and activity curve present how an athlete performed over a match quarter in terms of percentage time. For example, referring to Fig. 8, for 25 % of the match quarter, the high-pointer, HP1, can perform at 85 % of  $S_0$  or higher; and for 50 % of the match quarter, HP1 is at least 76 %  $S_0$ , and for the whole match quarter (100 %), HP1 can maintain more than 24 %  $S_0$ .

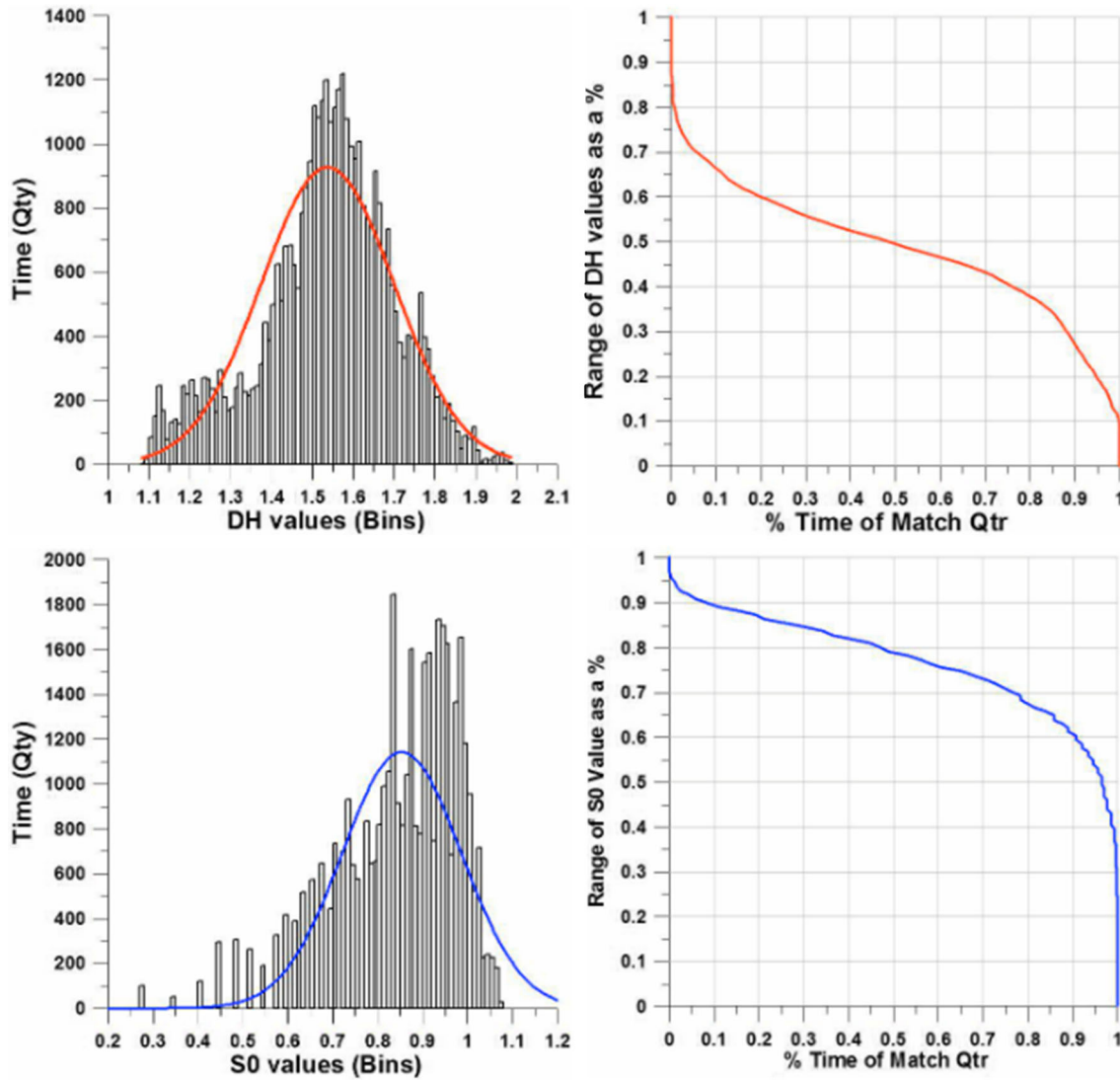


Fig. 7 Probability density and cumulative distribution plots of the  $S_0$  and  $D_H$  values

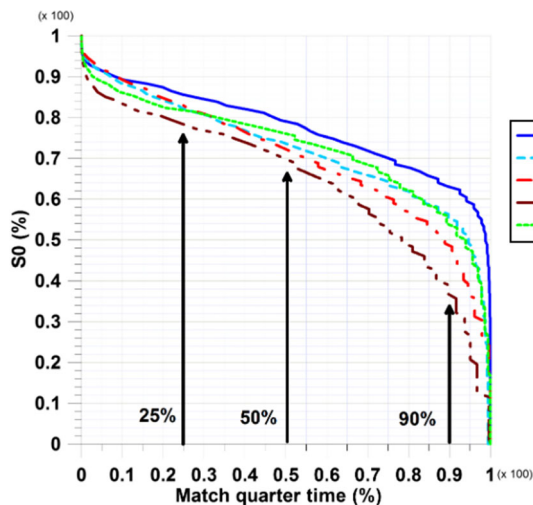


Fig. 8 Average performance curves of all five athletes based on  $S_0$

### 3.6 Mean activity duration analysis

Knowing how much time the athletes spend on each activity each time can provide more understanding of the athletes' output and performance. Each activity duration is the time an athlete spends on that activity before changing to the next activity. For example, an athlete might spend 5 s doing high-speed pushing followed by 5 s of high-speed coasting. Therefore, for each athlete classification (low-pointner, mid-pointner, and high-pointner), the activity durations of each of their five ranked activities were grouped together. As the distribution of the activity durations of each activity followed a Pareto distribution, the mean activity duration,  $\mu$ , was determined using the following equations:

For  $\alpha \leq 1$ ,



$$\mu = \infty \quad (10)$$

and for  $\alpha > 1$ ,

$$\mu = \frac{\alpha x_m}{\alpha - 1} \quad (11)$$

where  $x_m$  is the minimum possible time for an activity and  $\alpha$  is the shape parameter which is determined from the gradient of the distribution's logarithm plot.

## 4 Results

### 4.1 Performance and activity classification curves

Performance curves ( $S_0$  cumulative distribution plots) and activity curves ( $D_H$  cumulative distribution plots) were determined for every match quarter data. Average performance and activity curves for each athlete were also determined. In essence, the performance and activity curves revealed how the athletes performed over each quarter as a percentage. In general, the more convex the curve, the better the overall performance of that quarter.

Comparing the average performance curves (Fig. 8) of the athletes, it was clear that high-pointer HP1 had the best performance, while low-pointer LP1 had the lowest performance. It was not so clear-cut for the other athletes. Looking at 25 % of the match quarter, MP2 had higher performance followed by MP1 and LP2. At 50 % of the match quarter, it was LP2 first, followed by MP1 then MP2. Then, at 90 % of the match quarter, MP1 higher, followed by LP2 then MP2. This reveals that the mid-pointers had short bouts of higher performance, but over longer periods, their performance level became lower than the low-pointers. However, the high-pointer was definitely at a higher performance throughout the match quarters.

Comparing the average activity curves (Fig. 9) of the five athletes, MP1 had the best overall performance in terms of activity level. This was followed by LP2, while LP1 had the least. Between MP2 and HP1, MP2 was higher than HP1 for up to 52 % of the average match quarter, but their positions swapped after that. This result showed a contrast to the performance curves, where HP1 had better performance than the rest. In the activity curves, the mid-pointers (MP1 and MP2) showed higher activity levels for up to 52 % of the average match quarter. Only LP1 consistently produced the lowest performance curve ( $S_0$ ) as well as activity curve ( $D_H$ ).

### 4.2 Decision templates

For activity identification and ranking, four match quarter data of each athlete were analyzed. For each match quarter

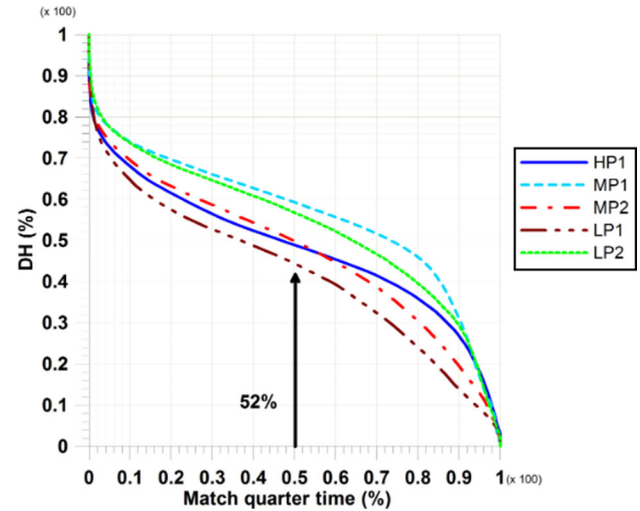


Fig. 9 Average activity curves of all five athletes based on  $D_H$

data, at least 30 known instances were identified as one of the five ranked activities, and tagged to the corresponding  $S_0$  and  $D_H$  data. These were then used to determine the boundary lines using the histogram method described earlier, which then produced five decision templates, as shown in Table 1.

Comparing the decision templates for the three classifications of athletes, there appeared to be a general trend of the boundary lines values dropping from the high-pointer to the low-pointers. For boundary line A (which separates ranked activities 1 + 2 + 3 and 4 + 5), there is an obvious downwards shift, as the classification of the athletes goes from high to low and also similarly between higher and lower competitive levels. This is in line with the fact that  $S_0$  is directly related to energy released. Therefore, Rank 4 and 5 activities for the high-pointer were of higher  $S_0$  values than the mid- and low-pointers; and comparing within the mid- and low-pointers, the athletes competing at a higher level also have higher  $S_0$  values for their Rank 4 and 5 activities.

### 4.3 Verification of activities ranking

Once the decision templates for each athlete were established, they can be applied to all the match data to determine the level of ranked activities in each match quarter. However, before continuing with the analysis of the level of ranked activities, the ranking had to be verified for its accuracy. This was carried out with one match quarter data by plotting the ranking and acceleration, and identifying by blocks of 50 data points where ranking was inconsistent with the activity as reflected by the acceleration signal. The result was an accuracy of 95.95 %.

#### 4.4 Comparison of ranked activities between athletes

After all the match activities were ranked, the numbers of data points for each ranked activity, of each match quarter, of all five athletes was tallied. The number of occurrences/instances of each activity for the average match quarter was calculated for each classification (high-pointer, mid-pointers, and low-pointers), and then expressed as a percentage of total amounts of activities in a match quarter. The duration of each instance of all five ranked activities, of all five athletes, was also tallied. It was found that the probability density of the activity duration followed a Pareto distribution instead of a normal distribution. Therefore, the mean duration of ranked activity was calculated based on the shape parameter ( $\alpha$ ) and the scale parameter ( $\beta$ ) of the Pareto distribution [32].

##### 4.4.1 Percentage of activities

Referring to Fig. 10, the percentage of activities plots reveals three distinct patterns:

- The high-pointer has more than 30 % of high-speed pushing but less high-speed coasting and only 10 % extreme collisions.
- The mid-pointers have almost similar amounts of high-speed pushing and high-speed coasting
- The low-pointers have the highest percentage of high-speed pushing (over 40 %) with less than 20 % for the other four activities.

The main difference that set them apart was the ratio of high-speed pushing to high-speed coasting or

pushing/coasting ratio (PCR). The low-pointers have the highest PCR of 2.33, followed by the high-pointer with a PCR of 1.3, and finally, the mid-pointers have a PCR of 0.97.

##### 4.4.2 Mean activity duration

Regarding the mean activity duration of all five ranked activities, Rank 1 activity had to be excluded from the comparison, because its mean value was indeterminable with the Pareto distribution's shape parameter ( $\alpha$ ) value of less than 1 [32]. Rank 5 was also excluded, because collision times are in reality very short. However, as the instances of each activity were identified using a running average window width of 2.5 s, each collision will include the time before and after the collision, and this can cause the mean duration to be extended.

Referring to Fig. 11, the low-pointers have the highest mean duration for low activity, while MP2 has the highest duration in high-speed coasting as well as high-speed pushing. The high-pointer has the lowest mean duration for all three activities. This is likely because the high-pointer can achieve higher accelerations and, thus, require shorter durations of high-speed pushing.

#### 4.5 Match analysis

The previous sections presented the performance curves, activity curves as well as activities ranking for each individual athlete, and the average for each functional classification. Compiling these data of different athletes who played in the same match quarters, coupled with match scores, can offer some insight to match performance.

**Fig. 10** Percentage of activities in a match quarter for all three classifications

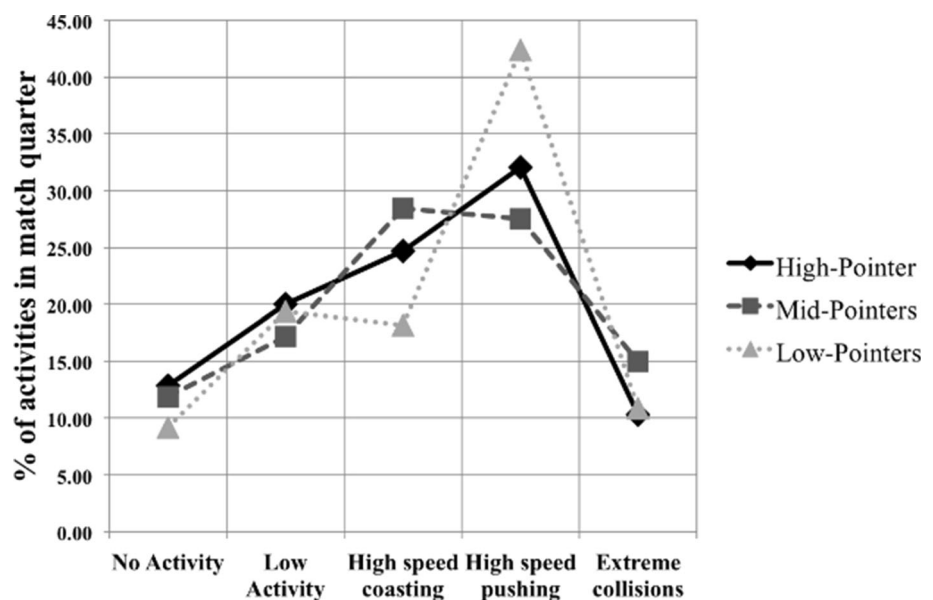


**Fig. 11** Mean duration of each activity, determined from a Pareto distribution; with coefficient of determination values in each column and the mean values on the *top*

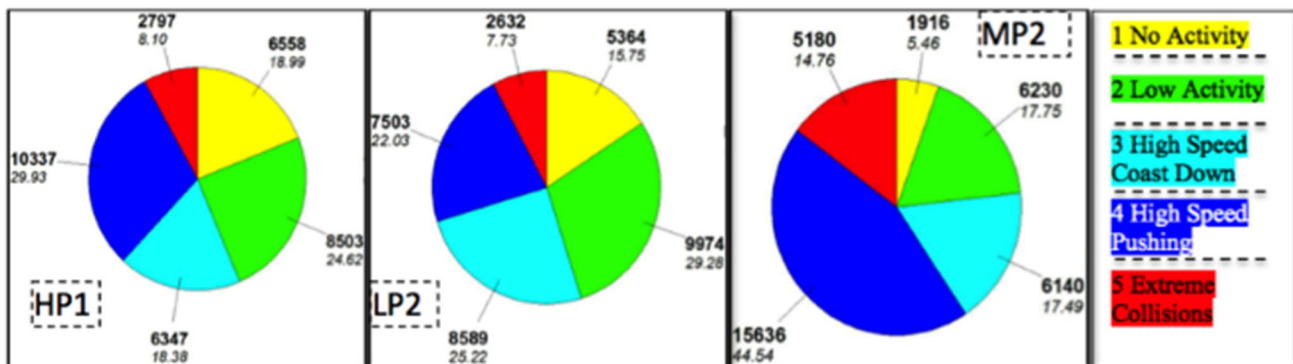
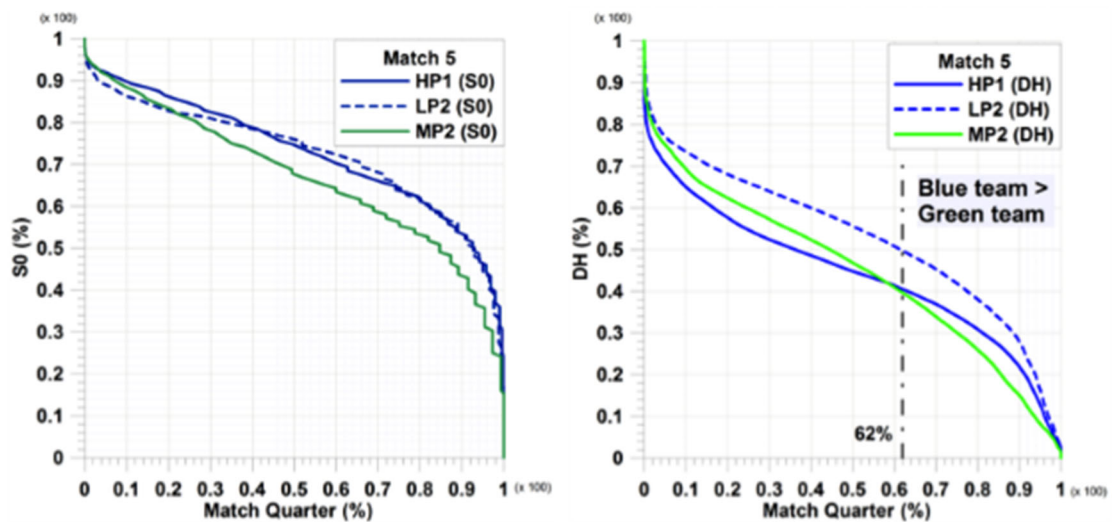
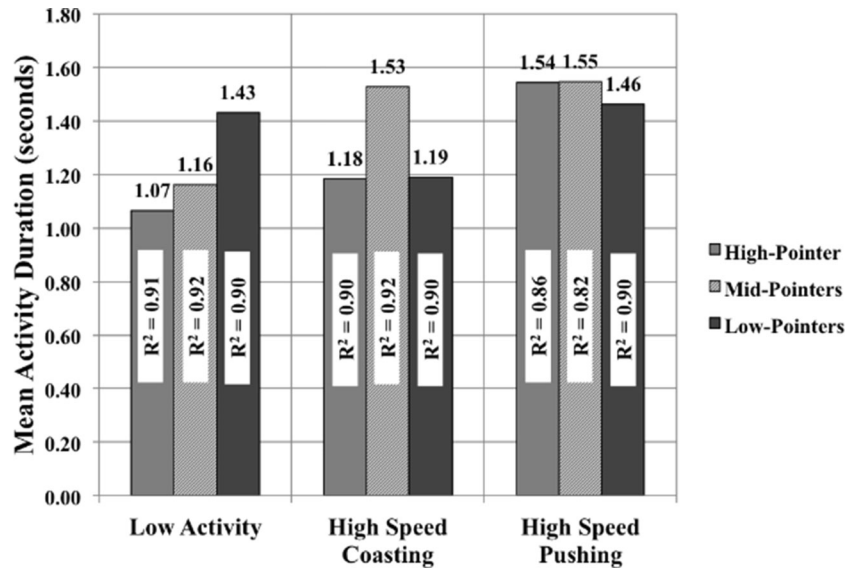


**Fig. 12** Match analysis of Match 5 using performance and activity curves and pie charts of ranked activities (yellow no activity, green low activity, light blue high-speed coasting, blue high-speed pushing, red extreme collisions) (color figure online)

In Match 5 (Fig. 12), three athletes were monitored: HP1, LP2, and MP2. HP1 and LP2 were in the blue team, while MP2 was in the green team. The final score was:

Blue team—29 and Green team—13. Comparing athletes in opposite teams: the Blue team had higher rating in performance ( $S_0$ ); and in terms of activity ( $D_H$ ), the Blue

team also rated higher for most of the match quarter (65–100 %). This supports the winning outcome of the Blue team. Comparing athletes in the same team (HP1 and LP2): they both had comparable results in terms of performance ( $S_0$ ), while LP2 rated higher in terms of activity ( $D_H$ ). Looking at their activities ranking, LP2 had the highest amount of high-speed pushing followed by HP1 then MP2, while MP2 had the most high-speed coast down.

In Match 6 (Fig. 13), three athletes were also monitored: HP1, LP2, and MP1, where HP1 and LP2 were in the Blue team, while MP1 was in the Black team. The final score was: Blue team—21 and Black team—31. Comparing athletes in opposite teams: all three athletes were comparable in performance ( $S_0$ ); but in terms of activity ( $D_H$ ), the Black team athlete rated higher for up to 90 % of the match quarter. Comparing athletes in the same team (HP1 and LP2): HP1 rated higher in terms of performance ( $S_0$ ), while LP2 rated higher in terms of activity ( $D_H$ ). Looking at their activities ranking, LP2 again had the highest amount of high-speed pushing followed by HP1 then MP1, while MP1

had the most high-speed coast down, even greater than high-speed pushing.

It is important to note that although the performance of the athletes seems to correlate to the final score of each match in this case; it is not an adequate representation, as only 3 out of 8 athletes were monitored. However, this suggests a possible method of analyzing a wheelchair rugby match.

## 5 Discussion

### 5.1 Factors that could influence performance of an athlete

Based on the results, it is possible to describe with some confidence three key attributes that can influence the performance of a wheelchair rugby athlete:

1. Functional classification—based on the assessment outlined by the International Wheelchair Rugby

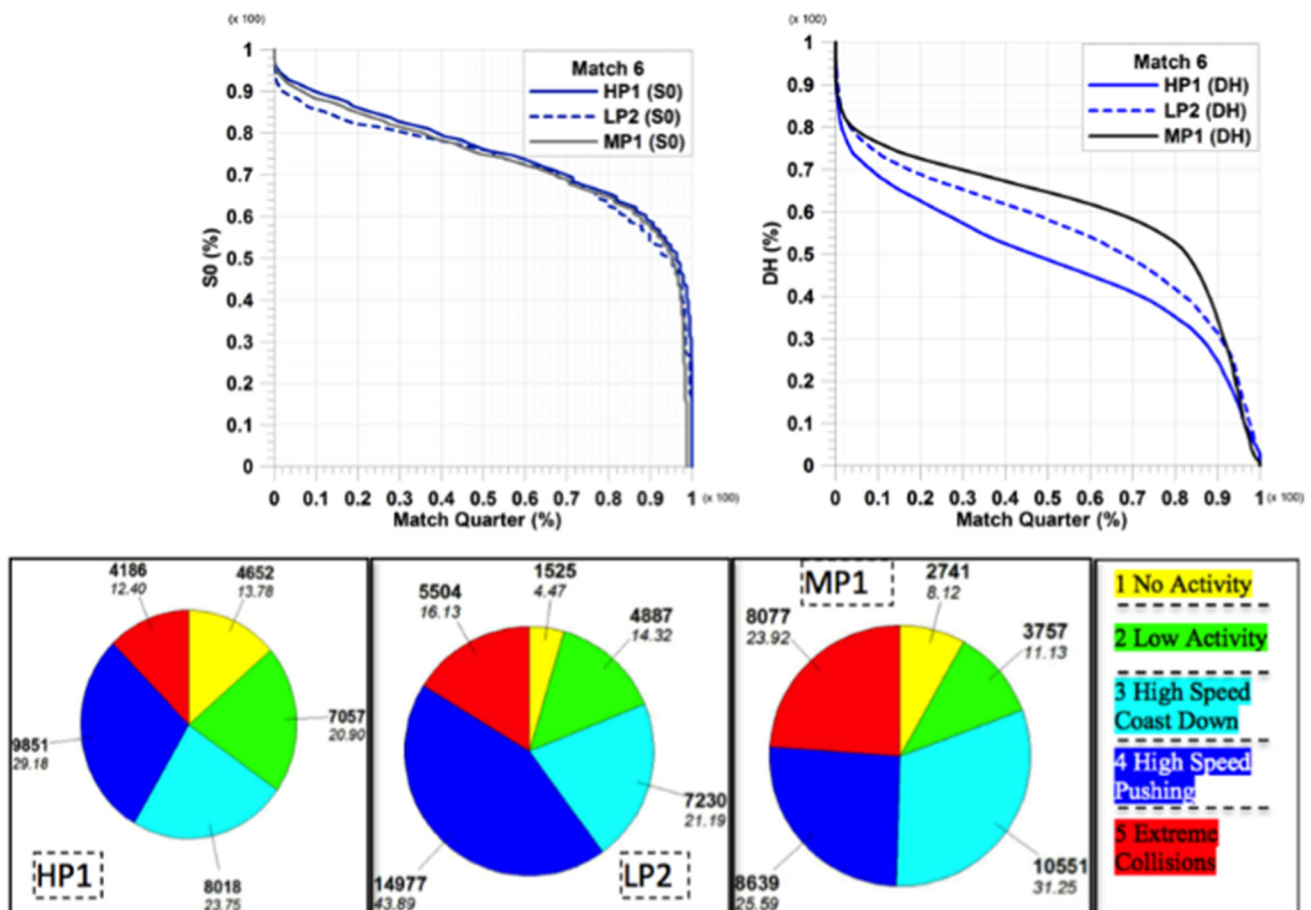


**Fig. 13** Match analysis of Match 6 using performance and activity curves and pie charts of ranked activities (yellow no activity, green low activity, light blue high-speed coasting, blue high-speed pushing, red extreme collisions) (color figure online)



Federation (IWRF) which is basically determined by physical capabilities and functional skills [33].

2. Level of training—as seen in this study, there are three levels of athleticism in the five observed athletes: Paralympics level, National level, and State level. Therefore, with more training and possibly talent, an athlete can improve in performance and, therefore, be able to move up to a higher level of competition; and
3. Design of a wheelchair—as the different classes of athletes play different roles during a match (either offensive or defensive or mix), their wheelchairs are also customized accordingly. For example, hi-pointer wheelchairs are typically designed to have higher maneuverability, while low-pointer wheelchairs have to be more stable and they usually have a more protruding pick bar for their defensive roles. The difference in design affects how fast the chair can go and its rolling resistance, and, therefore, the way the rugby wheelchair coasts down.

## 5.2 Ranked activities and classifications

With reference to Figs. 10 and 11, the different levels of ranked activities for the different classifications can be attributed to the three factors mentioned above.

### 5.2.1 Activity level comparison

Low-pointers have on average a higher percentage of high-speed pushing compared to the other two classifications. They need to push a lot more to keep their wheelchairs moving. They also have on average the lowest amount of high-speed coasting (Fig. 10). In terms of mean activity duration, the low-pointers' mean duration in high-speed pushing is close to the mean duration in low activity with a difference of 0.03 s on average. Their mean duration in high-speed coasting is only 1.18 s which is lowest comparing the three activities in Fig. 11. A main contributor to this outcome could be their wheelchair, which is designed with a bigger wheelbase for stability, has higher rolling resistance and, therefore, contribute to shorter coast downs.

On the other hand, the mid-pointers are slightly more mobile than the low-pointers; so if the low-pointers were unsuccessful at blocking or locking the opponents with their pick bar, the mid-pointers would attempt to chase the opponents and block them. This could lead to higher amounts of extreme collisions compared to the low-pointers who use locking tactics during defense.

The high-pointers tend to be in the offensive or ball-handling role. However, they also take up defensive roles depending on their position and situation. Typically, they try to maneuver away from opponents when they are trying

to score and will avoid collisions or blockages. It was observed that the high-pointer in this study had a higher percentage of high-speed pushing compared to high-speed coast downs; whereas the mid-pointers have quite similar levels of high-speed pushing and coast downs. This is likely due to the high-pointer having to make quick maneuvers or stoppages to avoid opponents instead of allowing the wheelchair to roll. The mean duration of the high-pointer's activities also show that the high-pointer spends more time on each high-speed pushing than high-speed coast down (Fig. 11).

### 5.2.2 Decision template trend

The combined application of  $S_0$  and  $D_H$  for identifying the five ranked activities was proven successful. Since the decision template was determined for each athlete individually, the amount of each ranked activity that was determined using the template did not reflect the intensity or effort put in by the athlete for that activity, as the ranked activities were all normalized. A comparison of the decision templates (Table 1) does reveal a linear trend with functional classification. However, this is inconclusive, as the sample size of athletes is too small.

## 5.3 Performance and activity curves

It was presented earlier that the performance curve which is based on running average  $S_0$  values represents the energy released by the athlete into the environment, while the activity curve is related to the activity performed by the athlete and push pattern. Referring to Fig. 3, which is a 2D mapping of activities and decision template belonging to the high-pointer, boundary line A separated Rank 1, 2, and 3 activities from Rank 4 and 5 activities. It was clearly a separation between low-energy activities from high-energy activities, which is what  $S_0$  represented. Then, boundary lines B and C separated the type of low-energy activities, while boundary line D separated the two different high-energy activities. In this case,  $D_H$  was able to separate different types of activities, but not on its own. Other than 'no activity', which is at the bottom of boundary line B,  $D_H$  alone could not separate the other activities. Therefore,  $D_H$  represents something else other than just Activity type.

In the analysis of Match 6, the match between the Blue team and the Black team; the performance curve (Fig. 13) showed that all three athletes—two from the Blue team and one from the Black team—had comparable performance, while the activity curve showed that MP1, the Black team athlete rated highest. The final outcome of the match where the Black team won by ten points was in line with the activity curve result. The activity curves of Match 5 also coincided with the final match outcomes. Thus,  $D_H$  could



have some correlation with performance-related parameters.

Prior to this study, two methods were used to acquire kinematic data of wheelchair rugby athletes during a match—a miniature data logger [2] and a video software tracking method [3, 34]. It was found in [2] that the high-pointers had higher average speeds than the rest. Coincidentally, the results of the overall performance curve ( $S_0$ ) in this study showed that the high-pointer had the best performance. Although  $D_H$  did not have a direct relation with wheelchair push patterns or wheelchair rugby activities, the activity curve based on  $D_H$  displayed possible relation with performance-related parameters. Furthermore, the outcome of the match comparisons showed that athletes from the winning teams had more convex performance and activity curves (which coincided with better performance), which suggested their potential application as performance measuring tools.

## 5.4 Relevance to the wheelchair rugby coach

### 5.4.1 Strategizing or match planning

The performance curve informs the coach of how much energy each athlete is able to generate and release throughout each match quarter and how long an athlete is able to maintain a certain amount of high-energy output (e.g., HP1 can maintain at least 80 %  $S_0$  for up to 40 % of the average match quarter, Fig. 8). Therefore, if performance data are processed and available at the end of each match quarter, the coach can determine if the athletes' performance is declining and make a decision on substitution for subsequent match quarters. The activity curve can be applied in the same manner.

### 5.4.2 Talent identification

The decision template derived for each athlete (Table 1) showed that there is a relation in classification, skill (competitive level), and the values of the decision template. This can potentially be a useful tool for talent identification (TID). Therefore, for example, if an athlete is only playing at the state league or state-level competition, but their decision template is as high as athletes playing in the national league or paralympic games, it could mean that they have the potential to play at a higher level and should be selected to train with the higher level teams. Greater sampling will be required to support this notion.

### 5.4.3 Match analysis with activity ranking

The most obvious statistic after a match is the score. However, the score of the match does not tell whether

each athlete was playing well or not. A coach can use video analysis software to tag the instances in the video where actions were positive (led to a score or blocked an opponent's score) or the opposite. Activity ranking gives the coach even more insight to the overall activities of an athlete during a match quarter—what distribution of activities among the athletes led to a win or a loss. For example, in comparing Match 5 and 6 data (Figs. 12 and 13), the Blue team won Match 5 against Green team but lost Match 6 against Black team. The mid-pointers of the Green and Black teams (MP2 and MP1) who played the same role in their team were analyzed and compared. The comparison outcome showed that MP1 produced more extreme collisions, high-speed pushing and high-speed coast downs than MP2, and at the same time, less low activities and no activities than MP2. This could be one of the contributing factors to Black team winning in match 6.

## 5.5 A note on the cumulative distribution plot

The performance and activity curves were cumulative plots determined from probability density functions of the continuous  $S_0$  and  $D_H$  data (Fig. 7). The application of cumulative plots for profiling, for example, is used for characterizing surface roughness by means of the Abbott–Firestone curve.

## 6 Conclusion

The main objective of this study was to develop an optimal method to identify and rank activities of wheelchair rugby athletes on the court. Two different methods of obtaining Fractal dimensions were used in a complementary way to identify different types of activities in wheelchair rugby. The calculations of  $S_0$  and  $D_H$  were also optimized with the most suitable  $w$  and  $m$  values. The quantified ranked activity of each athlete using the automated 2D mapping method was verified by visual inspection of the acceleration signal and comparison with synchronized video footage. The automated method was accurate in identifying 95 % of the activities.

The ranking outcome revealed differences between the three different functional classifications of the wheelchair rugby athletes. This could be related to their functional abilities, skills, and wheelchair design. However, the main limitation of this study is that it only analyzed five different wheelchair rugby athletes. It is recommended that for future studies, acceleration data of a larger population of athletes be collected. Then, the analysis methods developed in this study can be applied to further validate the match and performance analyses described earlier. When

validated, these methods can then serve as practical coaching tools for strategizing, talent identification, as well as post-match analysis.

**Acknowledgments** The authors would like to thank Disability Sport and Recreation for coordinating the data collection during the Victorian Wheelchair Rugby State League, as well as the athletes who volunteered to have their wheelchairs fitted with the mobile devices for this study. This work was supported by the Royal Melbourne Institute of Technology. The authors report no conflict of interest.

## References

- Rhodes J et al. (2014) The validity and reliability of a novel indoor player tracking system for use within wheelchair court sports. *J Sports Sci* 32(17):1639–1647
- Spörner ML et al (2009) Quantification of activity during wheelchair basketball and rugby at the National Veterans Wheelchair Games: a pilot study. *Prosthet Orthot Int* 33(3):210–217
- Sarro KJ et al. (2010) Tracking of wheelchair rugby players in the 2008 Demolition Derby final. *J Sports Sci* 28(2):193–200
- Hedley M et al (2010) Wireless tracking system for sports training indoors and outdoors. *Engineering of sport 8: engineering emotion*. In: 8th conference of the international sports engineering association (Isea). 2(2): 2999–3004
- Molik B et al (2008) An examination of the international wheelchair rugby federation classification system utilizing parameters of offensive game efficiency. *Adapt Phys Act Q* 25(4):335–351
- Morgulec-Adamowicz N et al (2010) Game efficiency of wheelchair rugby athletes at the 2008 Paralympic games with regard to player classification. *Human Mov* 11(1):29–36
- Gabbett TJ et al (2013) Relationship between tests of physical qualities and physical match performance in elite rugby league players. *J Strength Cond Res* 27(6):1539–1545
- Montgomery PG, Pyne DB, Minahan CL (2010) The physical and physiological demands of basketball training and competition. *Int J Sports Physiol Perform* 5(1):75–86
- Boyd LJ, Ball K, Aughey RJ (2011) The reliability of MinimaxX accelerometers for measuring physical activity in Australian football. *Int J Sports Physiol Perform* 6(3):311–321
- Davey N, Anderson M, James DA (2008) Validation trial of an accelerometer-based sensor platform for swimming. *Sports Technol* 1(4–5):202–207
- Dencker M et al (2010) Objectively measured daily physical activity related to aerobic fitness in young children. *J Sports Sci* 28(2):139–145
- Wickel EE, Eisenmann JC, Welk GJ (2009) Maturity-related variation in moderate-to-vigorous physical activity among 9–14 year olds. *J Phys Act Health* 6(5):597–605
- Tanaka C, Tanaka S (2009) Daily physical activity in Japanese preschool children evaluated by triaxial accelerometry: the relationship between period of engagement in moderate-to-vigorous physical activity and daily step counts. *J Physiol Anthropol* 28(6):283–288
- Bojic T, Vuckovic A, Kalauzi A (2010) Modeling EEG fractal dimension changes in wake and drowsy states in humans—a preliminary study. *J Theor Biol* 262(2):214–222
- Kulish V, Sourin A, Sourina O (2006) Human electroencephalograms seen as fractal time series: mathematical analysis and visualization. *Comput Biol Med* 36(3):291–302
- Weiss B et al (2009) Spatio-temporal analysis of monofractal and multifractal properties of the human sleep EEG. *J Neurosci Methods* 185(1):116–124
- Paramanathan P, Uthayakumar R (2008) Application of fractal theory in analysis of human electroencephalographic signals. *Comput Biol Med* 38(3):372–378
- Phothisonothai M, Nakagawa M (2008) EEG signal classification method based on fractal features and neural network. *Conf Proc IEEE Eng Med Biol Soc* 2008:3880–3883
- Fuss FK, Niegl G (2009) Instrumented climbing holds and performance analysis in sport climbing. *Sports Technol* 1(6):301–313
- Chua JJC et al (2010) Wheelchair rugby: fast activity and performance analysis. *Engineering of sport 8: engineering emotion*. In: 8th Conference of the international sports engineering association (Isea). 2(2):3077–3082
- Fuss FK, Subic A, Chua JJC (2012) Analysis of wheelchair rugby accelerations with fractal dimensions. *Procedia Eng* 34:439–442
- Hausdorff F (1919) Dimension und äußeres Maß. *Math Ann* 79(1–2):157–179
- Fuss FK (2013) A robust algorithm for optimisation and customisation of fractal dimensions of time series modified by nonlinearly scaling their time derivatives: mathematical theory and practical applications. *Comput Math Methods Med* 2013:1–19
- Rényi A (1955) On a new axiomatic theory of probability. *Acta Math Hung* 6(3–4):285–335
- Katz MJ (1988) Fractals and the analysis of waveforms. *Comput Biol Med* 18(3):145–156
- Higuchi T (1988) Approach to an irregular time series on the basis of the fractal theory. *Phys D* 31:277–283
- Rényi A (1960) On measures of information and entropy. In: 4th Berkeley symposium on mathematics, statistics and probability. Statistical Laboratory of the University of California, Berkeley, pp 547–561
- Schroeder MR (1991) Fractals, chaos, power laws: minutes from an infinite paradise. Dover Publications, Mineola, New York, pp 203–224
- Esteller R et al (2001) A comparison of waveform fractal dimension algorithms. *IEEE Trans Circuits Syst I Fundam Theory Appl* 48(2):177–183
- Gnitecki J, Moussavi Z (2003) Variance fractal dimension trajectory as a tool for heart sound localization in lung sounds recordings. In: Proceedings of the 25th annual international conference of the IEEE engineering in medicine and biology society, vols. 1–4, 25: pp 2420–2423
- Kulish V (2004) Partial differential equations. Pearson/Prentice Hall, Upper Saddle River, New Jersey, p 180
- von Seggern D (1993) Pareto probability density, in CRC standard curves and surfaces. CRC Press Inc, Boca Raton, p 252
- Hart A et al (2011) IWRF classification manual. International Wheelchair Rugby Federation, Canada, 3rd Edition Revised. [http://www.iwrf.com/resources/iwrf\\_docs/IWRF\\_Classification\\_Manual\\_3rd\\_Edition\\_rev-2011\\_\(English\).pdf](http://www.iwrf.com/resources/iwrf_docs/IWRF_Classification_Manual_3rd_Edition_rev-2011_(English).pdf). Accessed 7 July 2016
- Sarro KJ et al. (2010) Correlation between functional classification and kinematical variables in elite wheelchair rugby players. In: Jensen R et al. (eds) International symposium of biomechanics in sports, Marquette, University of Konstanz, Germany, pp 124–125